Fetal Chest

4

Dorothy Bulas and Alexia Egloff

Ultrasonography (US) is the screening method of choice for the evaluation of the fetal airway and chest. It is safe, inexpensive, and easily performed. Advances in US technique including higher resolution transducers, Doppler, and 3D/4D imaging have allowed for improved assessment of the congenital thoracic masses. The assessment of the fetal chest by US, however, is operator dependent and evaluation may be limited due to fetal position, maternal obesity, overlying bone, and/or oligohydramnios. Ultrasound evaluation is sensitive in the diagnosis of many prenatal lung lesions but has low specificity [1].

Magnetic resonance imaging (MRI) is an alternative modality that uses no ionizing radiation, has excellent tissue contrast and a large field of view, is not limited by obesity or overlying bone, and can image the fetus in multiple planes regardless of fetal lie. Faster scanning techniques allow studies to be performed without sedation in the second and third trimester with minimal motion artifact. Fetal MRI helps confirm the presence of masses identified by US, can delineate anatomy such as the trachea not visualized by US, more accurately measure lung volumes, and may demonstrate additional subtle anomalies. Experts in fields such as pediatric surgery and neonatology not comfortable interpreting US imaging can provide additional expertise when reviewing MR images. This multidisciplinary approach is crucial for the success of handling these complex cases [2–5].

Thus, advances in both US and MRI have improved our ability to accurately diagnose fetal airway and chest anomalies and furthered our understanding of the evolution of fetal lung lesions.

D. Bulas (✉)
Department of Diagnostic Imaging and Radiology, George Washington University Medical Center, Children's National Medical Center, Washington, DC, USA
e-mail: dbulas@cnmc.org

A. Egloff
Department of Radiology, Children's National Medical Center, Washington, DC, USA

The prenatal and postnatal prognosis for fetuses with chest anomalies is quite variable. Fetal imaging not only is important for the initial diagnosis of the lesion but is also useful for follow-up in case nonimmune hydrops develops. Preparation for delivery at a tertiary institution is critical for the fetus with a large airway or chest mass. The decision to perform in utero intervention or an ex utero intrapartum treatment (EXIT) delivery places both the mother and fetus at risk and thus benefits from precise evaluation and accurate assessment of the situation. Prenatal evaluation not only allows for the planning of in utero therapy but can optimize postnatal therapeutic planning with reduction in neonatal imaging, useful when caring for the unstable infant [2–4].

Prenatal diagnosis does not always result in improved outcome as some cases are associated with lethal pulmonary hypoplasia. A small chest mass can be associated with severe chromosomal anomalies or other lethal anatomic abnormalities. Thus, accurate chromosomal and structural assessment of the entire fetus is also important for appropriate counseling and planning of in utero interventional procedures, delivery, and postnatal management.

Ultrasonography Imaging of the Fetal Neck and Chest

Ultrasonography of the Fetal Chest

Ultrasound is the initial imaging modality in the detection of fetal chest masses. On axial images, the normal fetal chest is oval or round. The heart is positioned within the anterior half of the left chest and bordered on both sides by lung tissue. The apex of the heart touches the wall of the left anterior chest, while the intersection of the atrial septum with the posterior heart border lies just to the right of center. The lungs, thorax, and heart grow proportionally, so the normal cardiothoracic ratio is constant throughout the pregnancy, and the cardiac position and axis should not change over time. The fetal ribs are echogenic and encompass more than

R. H. Cleveland, E. Y. Lee (eds.), *Imaging in Pediatric Pulmonology*, https://doi.org/10.1007/978-3-030-23979-4_4

half the chest circumference on either side. The ultrasound appearance of normal fetal lungs is typically homogeneous and echogenic. In early pregnancy, the lungs are less echogenic than the liver, but echogenicity increases through gestation as the lungs become more fluid filled. At times, the echogenicity of the lung may appear similar to the adjacent liver and bowel making it difficult to differentiate sonographically from the surrounding organs. Inferiorly, the diaphragms border the lungs and are dome shaped and hypoechoic. It is important to remember that visualization of a seemingly intact diaphragm does not exclude a diaphragmatic hernia as a small defect may be missed. The thymus, a homogeneous anterior mediastinal structure, is often not well seen because of overlying rib shadowing. Normal measurements for the fetal thymus have been published. A smaller than normal-sized thymus can be seen in fetuses with intrauterine growth restriction, Down syndrome, congenital heart defects in combination with 22q11 microdeletion, preeclampsia, and preterm rupture of membranes [6].

Different two-dimensional measurements have been used to assess lung development for age. The chest circumference measured at the level of the four-chamber view of the heart has been traditionally used. A recent study by Britto et al. suggests using 3D ultrasound to estimate chest circumference by using the fetal aorta and inferior angle of the scapula as anatomical landmarks [7]. This approach should provide a better assessment of lung and thorax development as landmarks are less likely to be affected or displaced by thoracic pathology compared to the heart. Three-dimensional US can also provide lung volumetry measurements [8]. Nomograms exist for chest circumference, 2D oblique lung diameter and 3D volumetry [7–9], and can be used to aid in the early diagnosis of pulmonary hypoplasia. Obtaining volume measurements, however, can be difficult in all three planes as oligohydramnios, maternal obesity, or fetal lie may make differentiation of the lung and surrounding structures difficult.

Sonographically, congenital lung masses can appear hypoechoic/cystic or hyperechoic/microcystic/solid and small or large (Fig. 4.1). When a solid lung mass is present, the echogenicity may be similar to adjacent liver and lung and, thus, difficult to identify. Shift of the heart and flattening of the diaphragms may be the first clue that a lung mass or diaphragmatic hernia is present (Fig. 4.2). Echogenic masses may become less visible later in gestation as the surrounding lung tissue becomes more echogenic and rib shadowing increases. The differential for lung masses includes congenital diaphragmatic hernia (CDH), congenital pulmonary airway malformation (CPAM/CCAM), bronchopulmonary sequestration (BPS), congenital lobar emphysema (CLE)/bronchial atresia, hybrid lesions, and congenital hydrothorax [10–12]. Ultrasound while sensitive in the identification of many lung lesions due to their abnormal echogenicity and/or mass affect has a low specificity [1].

Ultrasonography of the Fetal Neck

Ultrasound imaging the fetal neck is also important in the assessment of the fetal airway and lungs. Axial images of the neck may demonstrate the larynx and pharynx sonographically if they are fluid filled, but the trachea is typically not visualized. Axial images of the posterior neck are important for the identification of nuchal translucency at 11–14 weeks and nuchal thickening at 16–20 weeks both of which are markers for aneuploidy. The jugular vein and carotid artery can be identified by color Doppler and may be deviated if a mass is present. A detailed exam of the neck is not always possible by ultrasound when oligohydramnios, maternal obesity, or fetal lie prevents adequate visualization. If the neck is in fixed extension, there should be concern that a neck mass is present.

When a neck mass is identified, internal characteristics may help determine the diagnosis. There are a wide variety of neck masses which can be cystic (lymphatic malformation (lymphangioma/cystic hygroma), branchial cleft cyst, thyroglossal duct cyst, laryngocele, cervical meningomyelocele), solid (goiter, neuroblastoma, fibroma), or complex (teratoma, hemangioma, goiter). The two most common causes for neck masses are lymphangioma and teratomas [13] (Figs. 4.3 and 4.4).

The prognosis of a cervical mass is dependent on the amount of airway compression, presence of other anomalies, and development of hydrops. As the airway is not directly seen by US, secondary signs of airway compression such as polyhydramnios or a small stomach may suggest severity of airway compromise.

Magnetic Resonance Imaging of the Fetal Neck and Chest

Fetal Magnetic Resonance Technique

Advances in MR including single-shot rapid acquisition with relaxation enhancement sequences have significantly decreased movement artifact on 1.5 T and 3 T magnets. Slices are acquired individually with each slice obtained by a single excitation pulse taking less than 400 ms. A series can be obtained in less than 30–40 seconds with slices as thin as 2–3 mm. These T2-weighted images have excellent contrast and spatial resolution and good signal-to-noise ratios. Sequences available include single-slice fast spin echo, ssFSE (GE, Milwaukee, WI), and half-Fourier acquisition single-shot turbo spin echo, HASTE (Siemens, Erlangen, Germany) [14, 15]. Additional MR sequences include heavy T2w hydrography, fast T1w sequences including fast multiplanar spoiled gradient echo, diffusion-weighted sequences, and two-dimensional fast low angle shot. These sequences

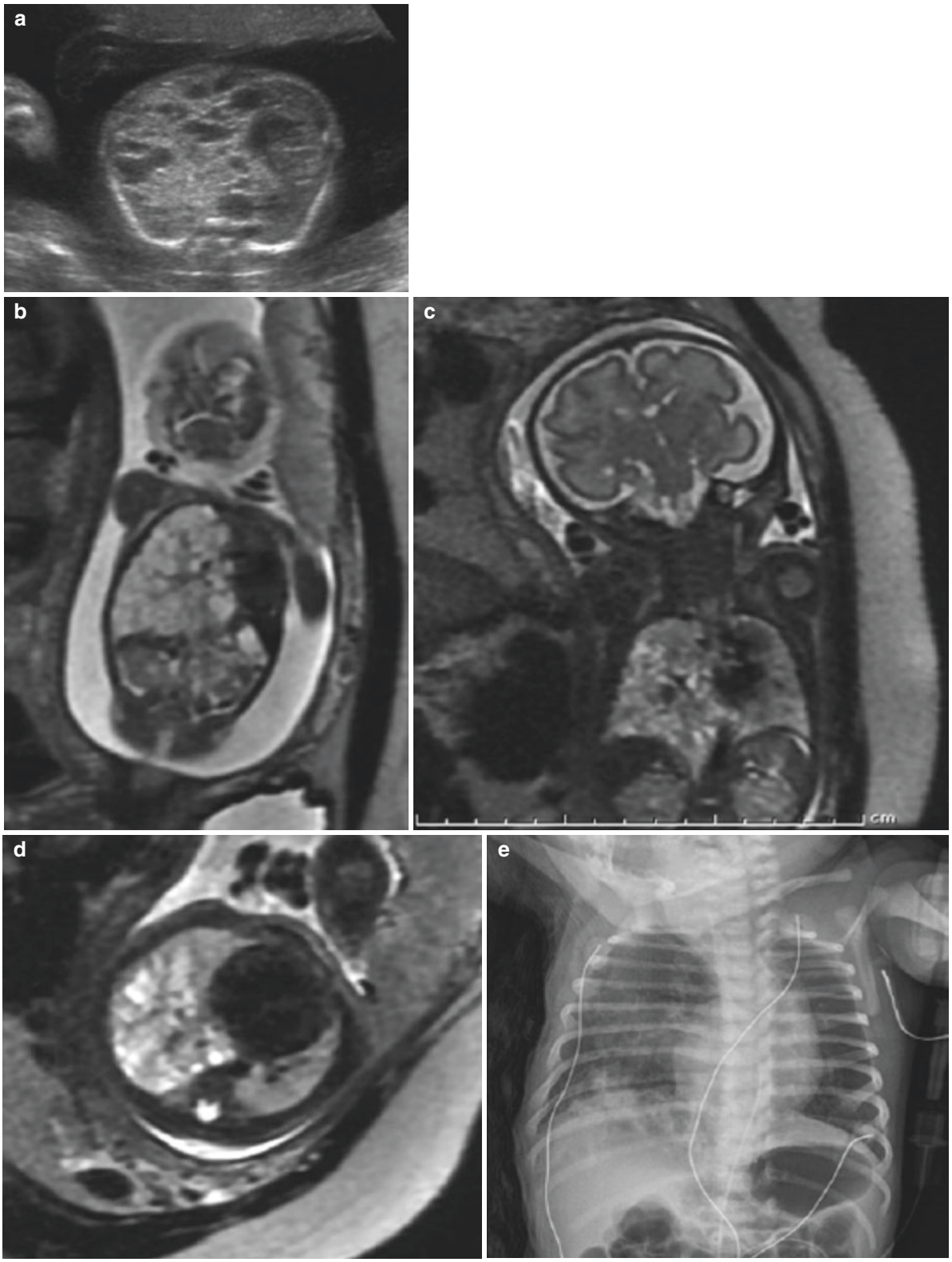

Fig. 4.1 Congenital pulmonary airway malformation. (**a**) Axial US at 21 weeks gestation demonstrates a large mixed macrocystic and microcystic mass in the right hemithorax with compression of normal left lung. (**b**) Coronal SSFSE T2w MR image also at 21 weeks confirms the presence of a large multicystic mass in the right hemithorax everting the diaphragm inferiorly and deviating the heart to the left. The CPAM volume ratio (CVR) measures 2.4 high risk for developing hydrops. Follow-up coronal (**c**) and axial (**d**) MR images at 30 weeks gestation demonstrates growth of the fetus with stable size of the right lung mass. The mass no longer everts the diaphragm nor deviates the heart to the left. The CVR has improved and now measures 1.4 low risk for developing hydrops. (**e**) At delivery, the infant had minimal respiratory distress. Chest radiograph demonstrates minimally heterogeneous right lower lobe

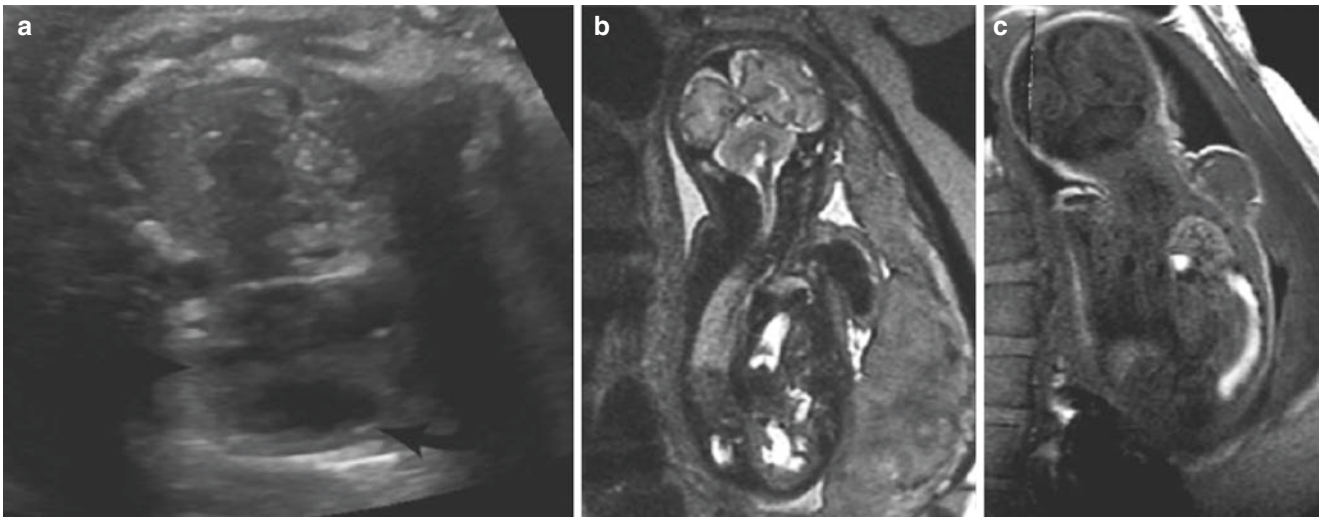

Fig. 4.2 Congenital diaphragmatic hernia. (**a**) Axial US of a fetal chest demonstrates a heterogeneous mass in the left hemithorax deviating the heart (*curved arrow*) to the right. (**b**) Coronal SSFSE T2w image of the fetal chest demonstrates that small and large bowel is herniated into the left hemithorax consistent with a diaphragmatic hernia rather than CPAM. (**c**) Coronal T1w image confirms that high-signal meconium filled bowel and liver are herniated into the left hemithorax

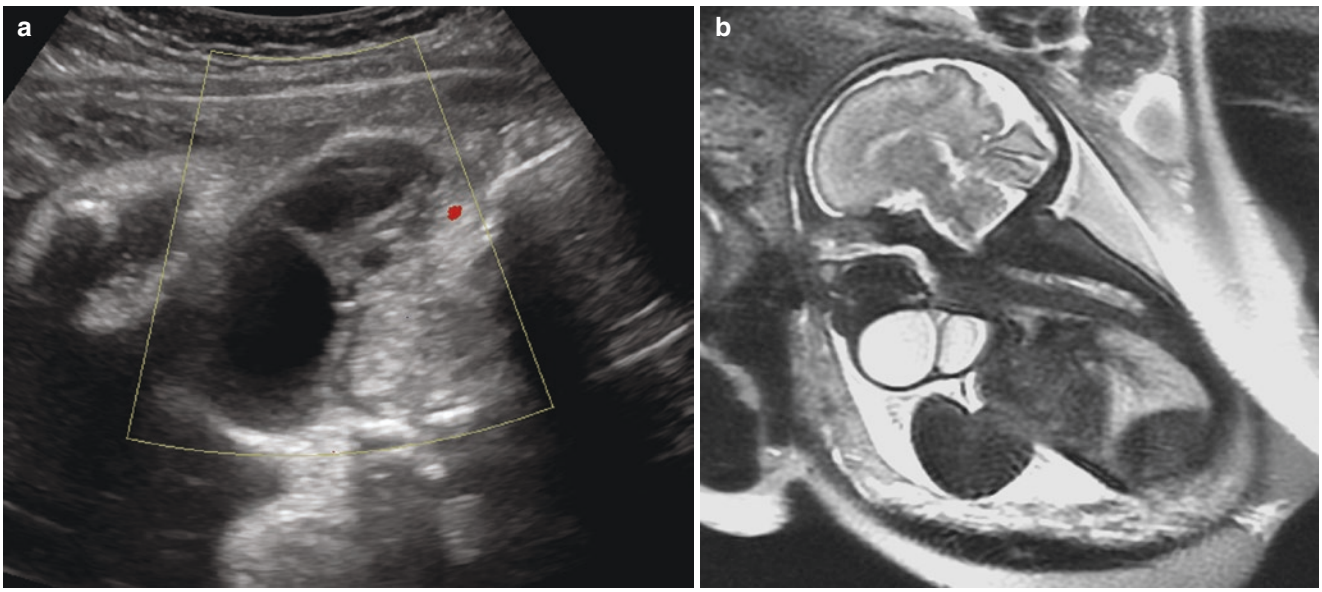

Fig. 4.3 Cervical lymphangioma. (**a**) Axial US image of the fetal neck demonstrates several macrocysts with no significant vascularity. (**b**) Sagittal SSFSE T2w MR image of the fetal neck at 30 weeks' gestation confirms the presence of a large multiseptated mass compressing the cervical trachea

take longer and may require breath holding and thicker slices for sufficient signal-to-noise ratios.

Total study time can average 20–40 min, depending on fetal movement which is particularly problematic in cases of polyhydramnios and younger gestations. Studies may be limited due to maternal size, claustrophobia, and maternal discomfort in the supine position. Left lateral decubitus position can be helpful in patients with back pain or with supine hypotension. A fast multiplanar spoiled gradient-echo sequence or large field of view (48 cm; section thickness 8 mm; intersection gap 2 mm) coronal ssFSE localizer is first performed to evaluate fetal position and select future imaging planes. Each subsequent plane is placed orthogonal to the previous sequence to account for fetal movement. Axial, sagittal, and coronal T2w images angled to the fetal chest are obtained at 3–5 mm thickness, 0 mm section gap. Planes angled to the fetal brain and abdomen are important for complete assessment of the fetus. Quiet maternal breathing is adequate for

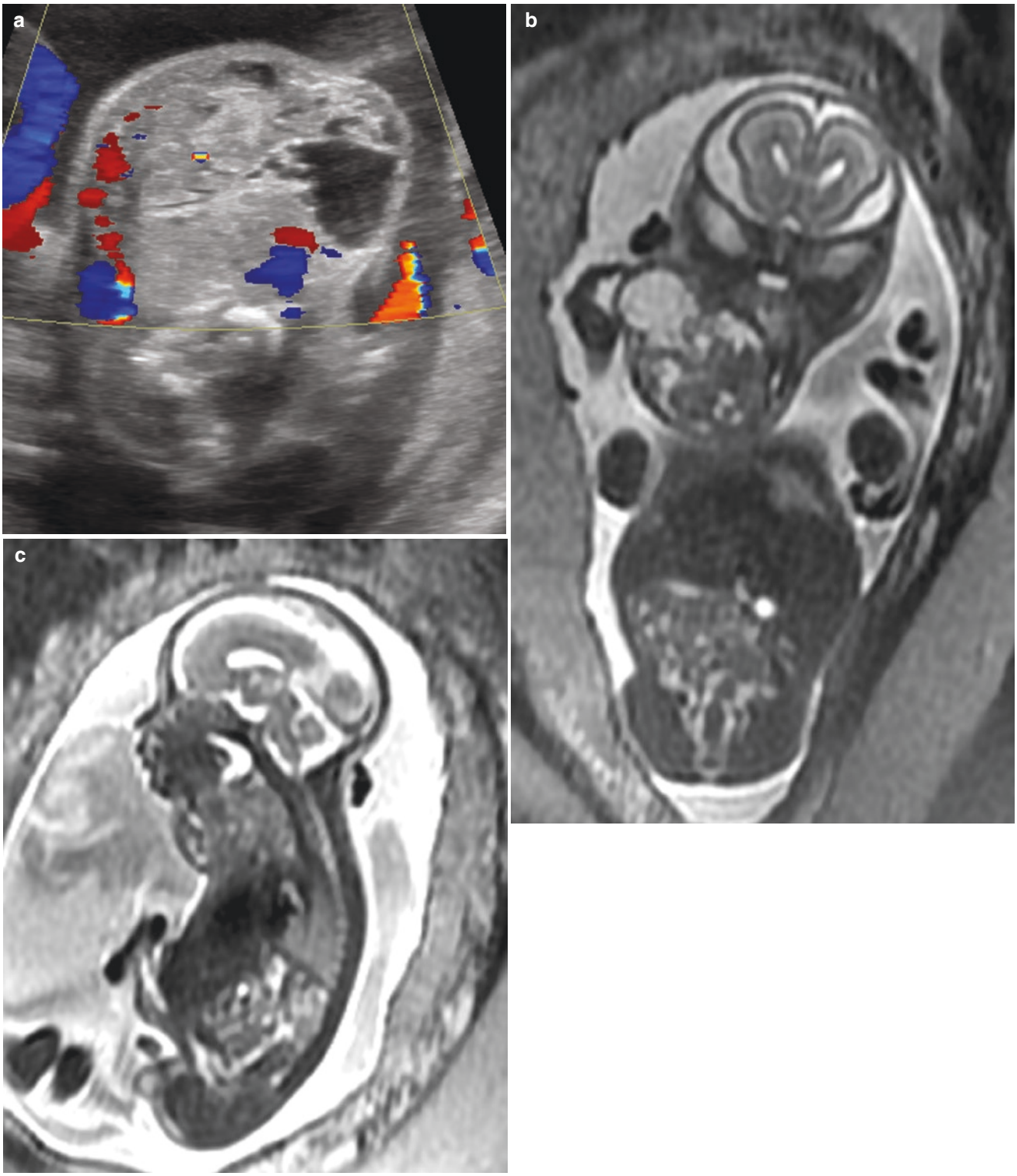

Fig. 4.4 Cervical teratoma. (**a**) Axial US image of the fetal neck at 21 weeks' gestation demonstrates a mixed cystic and solid mass with prominent vessels. Coronal (**b**) and sagittal (**c**) fetal T2w MR images confirm the presence of a large mass compressing the cervical trachea. The oropharynx was distended with fluid. Polyhydramnios was present

T2w images, with breath-hold T1w, echoplanar, and angiographic sequences added as needed. Fetal MRI provides improved anatomic evaluation of the airway and lungs, helps corroborate the diagnosis, and often provides additional information useful for management planning including fetal intervention [2, 3]. More specific diagnosis prenatally provides improved counseling, decreasing the level of stress that could result when a thoracic anomaly is diagnosed [5].

Fetal Magnetic Resonance Safety

There is no definitive evidence that MRI produces harmful effects on human embryos or fetuses using current clinical parameters. The long-term safety of MRI exposure to the fetus, however, has not been definitively demonstrated [16–18].There has been concern that prolonged exposure to high-field MRI may affect embryogenesis, chromosomal structure, or fetal development [3]. Animal studies on embryos have not demonstrated any growth abnormalities or genetic damage at clinical levels of exposure so far [19, 20]. There is concern that with higher strength units and prolonged scanning times, biological effects may occur if applied at sensitive stages of fetal development [21, 22]. Recently, the long-term safety after MRI exposure in the first trimester was assessed with a large retrospective study and demonstrated no significant increase in congenital anomalies, neoplasms, or vision or hearing loss [23].

Compliance with the US Food and Drug Administration (FDA) and International Commission on Nonionizing Radiation Protection (ICNIRP) guidelines requires control of specific absorption rate (SAR) values [24, 25]. Medical Device Agency (MDA) guidelines require control of the maximum SAR (10 g) within the fetus. The most frequently used sequences do operate at the SAR limit recommendations. These limits need to be carefully followed with higher field systems as well [26]. MR is not routinely recommended during the first trimester due to the small fetal size and significant fetal motion limiting imaging at this gestation .

Gadolinium should not be used with fetal imaging as it has been shown to cross the placenta. The fetus excretes and then swallows gadolinium which gets reabsorbed from the gastrointestinal tract. In animal studies, growth retardation has been reported after high doses of gadolinium (Magnevist product information, Berlex Labs, Wayne, NJ). A retrospective study demonstrated an increase in rheumatologic, inflammatory, or infiltrative skin conditions as well as stillbirths and neonatal death after gadolinium administration [23], Thus exposure of the fetus to gadolinium is not recommended.

MRI of the Fetal Chest

Fetal MRI is a useful adjunct in the assessment of the fetal airway and chest. Fluid in the trachea and larynx is high T2w and thus well delineated [27]. Fetal lungs are homogeneously brighter than muscle and increase in signal after 24 weeks' gestation due to the development of alveoli and production of alveolar fluid [28] in the third trimester. Normal lung when compressed by a mass may be slightly hypointense compared to noncompressed normal lung. Normal lung parenchyma is easily separated from abnormal lung masses which tend to be higher in signal.

The mediastinal structures, liver, and lung are easily differentiated by MR. The liver and spleen are low in signal on T2w with liver higher in signal on T1w than normal lung. On T2w, meconium is low in signal, while fluid-filled small bowel is high in signal. This reverses on T1w when meconium is bright and fluid-filled small bowel is low in signal and is easily distinguished from adjacent lung and liver in cases of CDH (Fig. 4.2). The thymus is homogeneous and of higher signal than the heart which appears as a flow void on T2w.

The ability to image in any plane and large field of view aids in the delineation of fetal lung masses. Lung volumes can be measured in any plane, and normative data are being accumulated for various gestational ages. Volumetric lung measurements appear to be reproducible and increase with gestational age. The right lung measures approximately 56% of the total lung volume. When oligohydramnios limits visualization of the fetus sonographically, MR can still demonstrate many anomalies, and lung volumes can be measured to assess for pulmonary hypoplasia. In complex cases, such as thoracopagus conjoined twins, the large field of view can be particularly helpful. Thus, while US is the initial modality in detecting chest masses, MRI is useful in confirming the presence of a mass, providing assessment of residual lung volume, and further characterizing the lesion increasing specificity.

MRI of the Fetal Airway

Prenatal evaluation of the fetal neck is difficult with complex embryology involving the development of vascular, lymphatic, musculoskeletal, and digestive systems. Masses such as teratomas and lymphangiomas can share both cystic and solid components, with precise histologic diagnosis difficult prenatally. If the neck mass is large and compresses the airway, death may occur at delivery if a patent airway is not established quickly. Thus, detection of a neck mass prenatally is important to prepare for the timing, location, and mode of delivery.

Fetal MRI is a useful adjunct in the evaluation of neck and thoracic masses which compress the fetal airway. The normal fetal airway can be visualized on T2w due to high-signal fluid within the larynx, trachea, and bronchi. The esophagus is not typically visualized but may be identified when distended by a distal obstruction. T1w images are useful for the diagnosis of a goiter which is of high signal on T1w.

When a neck mass is identified, MRI can delineate if the mass extends into the oropharynx. The amount of tracheal deviation and compression can be directly visualized. MRI is also useful for the evaluation of tracheal compression from thoracic masses. Mediastinal masses are rare and include foregut cysts, teratomas, esophageal duplication cysts, and bronchogenic cysts. Foregut cysts including bronchogenic, enteric, and neurenteric are typically fluid filled with high T2w homogeneous signal. Mediastinal teratomas have a complex heterogeneous appearance due to fat and fluid. These masses may compress the great vessels and result in hydrops and/or compress the esophagus and result in polyhydramnios [28].

The location of cystic and solid components of neck and mediastinal masses can be evaluated in three dimensions allowing the surgeon to plan for in utero intervention or post-delivery cyst aspiration or resection. If the fetus greater than 32 weeks' gestation with a large lesion expected to have difficulty breathing at delivery, EXIT may be considered. This partial delivery followed by intubation and intravenous access prior to clamping the umbilical cord can improve the survival of these difficult cases [29].

Prenatal Diagnosis and Management of Chest Anomalies

When an airway or chest abnormality is identified prenatally, several questions need to be answered:

- Are additional anomalies or hydrops present?
- Will there be pulmonary hypoplasia at delivery?
- Will there be airway obstruction at delivery?
- Can in utero intervention help?

The most common congenital thoracic lesions include CDH, congenital pulmonary airway malformation (CPAM/CCAM), BPS, congenital lobar overinflation/bronchial atresia, hybrid lesions, and congenital hydrothorax [30]. Pulmonary hypoplasia, agenesis, and aplasia are less common. A definitive diagnosis of a chest mass is usually possible only after surgical resection and histopathological evaluation [10–12].

In the fetus, the clinical importance of these lesions lies primarily in the mass effect on surrounding structures. This can result in compression of the airway, blood vessels, lymphatics and normal lung with development of pleural effusions, polyhydramnios, hydrops, and pulmonary hypoplasia. Outcome depends on the timing of secondary effects and severity of pulmonary hypoplasia. With improvement in fetal imaging, more aggressive fetal interventions have advanced. While the majority of cases with lung masses survive, masses that result in hydrops in the past were typically lethal. Now these masses may be amenable to fetal interventions such as maternal steroids, fetal thoracentesis, laser therapy, and in utero surgery [31–36].

Congenital Pulmonary Airway Malformation

Congenital pulmonary airway malformation (CPAM/CCAM) has varying appearances sonographically dependent on subtype. The pathologic classifications by Stocker et al. have no real prognostic value prenatally [37]. A simpler fetal classification by Adzick et al. [33] based on gross anatomy and imaging appearance has been recommended for prenatal assessment:

- Macrocystic – One or more macrocysts measuring >5 mm. These cysts are hypoechoic by ultrasound and high signal by MR. This subtype grows less rapidly but may develop hydrops and can require prenatal intervention (Fig. 4.5).

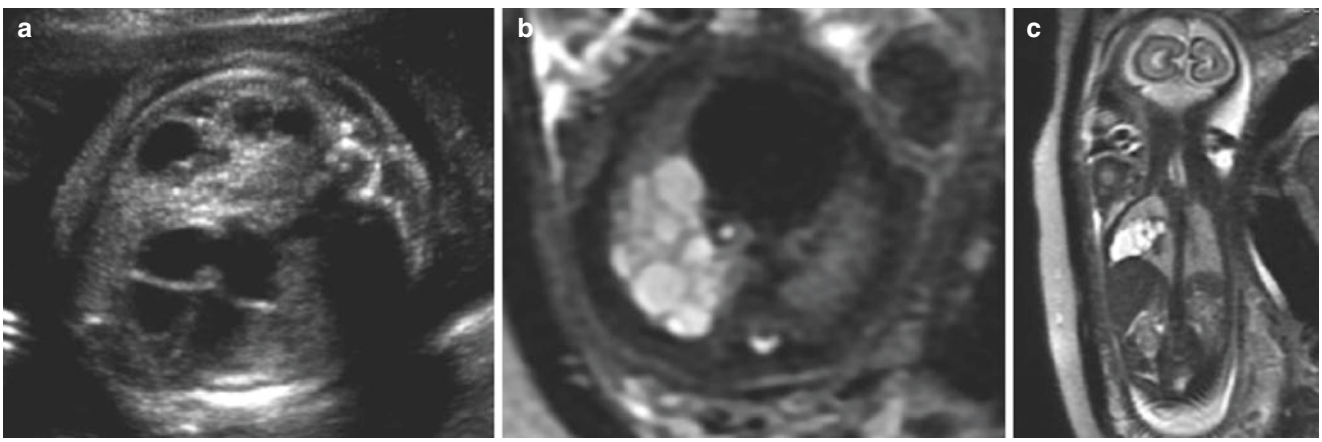

Fig. 4.5 Macrocystic CPAM. (**a**) Axial US image of the fetal chest demonstrates multiple macrocysts within the right hemithorax. Axial (**b**) and coronal (**c**) SSFSE T2w MR images confirm that the high-signal macrocysts are limited to the right middle lobe with normal intermediate signal right upper and lower lobe parenchyma

- Microcystic – Multiple microcysts <5 mm that appear homogeneously echogenic/solid by ultrasound and are high signal by MR. When large, they may be associated with mediastinal shift, pulmonary hypoplasia, polyhydramnios, and nonimmune hydrops requiring in utero intervention.

By ultrasound, macrocysts are well delineated from adjacent echogenic normal parenchyma. The microcystic subtype is echogenic as compared to normal lung but may become more difficult to visualize as gestational age advances due to the normal increase in echogenicity of surrounding normal lung as alveoli develop (Fig. 4.6). Shadowing from overlying ribs becomes more problematic in the third trimester limiting lung parenchymal visualization. When the mass is large, mediastinal shift can be identified by rotation and deviation of the heart axis.

When severe, vena cava and cardiac compression may result in hydrops, with pleural effusions, pericardial effusions, skin thickening, and ascites developing. Esophageal compression can result in a small stomach and polyhydramnios. Color and power Doppler imaging are useful in looking for a systemic feeding vessel [5], while 3D/4D imaging can be used to measure lung volumes [8].

By MR, CPAM are typically higher in signal than adjacent normal lung with mediastinal shift easily demonstrated. MR is particularly valuable when a rare bilateral CPAM is present. Lung volumes are easily measured in any plane by MR.

Prognosis does not depend on the type of lesion [33]; rather, it is dependent on the size of the mass, amount of mediastinal shift and pulmonary hypoplasia, fetal hemodynamics, associated anomalies, and gestational age at delivery [30, 33].

CPAM is rarely associated with chromosomal anomalies, but associated anomalies should still be searched for [34]. Karyotyping is not necessary if no other anomalies or risk factors are identified [34]. In the absence of hydrops, early survival without any intervention is higher than 95% [35].

Follow-up ultrasounds are critical to assess stability of mass size and the potential development of hydrops.]. The presence of hydrops is the most important indicator of poor outcome and can result in perinatal death approaching 100% without intervention [33].

A CPAM volume ratio (CVR) has been described as a predictor of hydrops and outcome [38]. It is obtained by calculating the volume of the lung mass and normalizing it by gestational age using the head circumference [38].

$$\text{CVR} = \frac{\text{height} \times \text{anteroposterior diameter} \times \text{transverse diameter} \times (\text{constant})}{\text{Head cirumference}}$$

If the CVR is less than 1.6, the risk of developing hydrops is low [38]. If the ratio is more than 1.6, the fetus is at high risk for developing hydrops, and intervention should be considered to increase survival.

CPAM typically show progressive growth between weeks 20 and 26 of gestation. By 26–28 weeks, growth begins to plateau. Usually, no hydrops develops after reaching the 28 weeks' growth plateau [38].

If hydrops develops and gestation is less than 32 weeks, various interventions have been attempted with the objective of decreasing fetal compromise and preventing lung hypoplasia [11]. Best approach is selected for each individual case depending on the presence of hydrops, the type of anomaly, and the consideration of potential risks of the various treatment options [39]. Interventions include maternal steroids, fetal thoracentesis, cyst aspiration, thoracoamniotic shunt, laser therapy, sclerotherapy, and in utero surgical resection [38–47].

Successful fetal surgery depends on surgical experience as well as optimal maternal anesthesia and uterine relaxation, hysterotomy, and fetal exposure techniques: intraoperative fetal monitoring, reliable amniotic membrane, and uterine closure. Close postoperative follow-up and early detection and treatment of preterm labor are fundamental. To undergo fetal surgery, maternal health needs to be considered to decrease the risk of complications [33].

Up to 50% of CPAM actually resolve prenatally [36]. Of the lesions that resolve in utero, 60% show no abnormality on postnatal imaging [36]. The remaining 40% with apparent prenatal resolution are still present postnatally but not well seen by follow-up prenatal imaging due to increase in normal lung echogenicity and difficulty in differentiating normal from abnormal lung [38]. When a persistent mass is seen, it is confirmed by postnatal imaging in over 95% of cases.

Persistent masses can decrease in size during the late second trimester [33] or have a relative decrease in size due to normal fetal growth. Some do actually increase in size. Implications for delivery and postnatal management include size of mass at delivery and the presence of hydrops. If the lesion is small with no hydrops, the obstetrician and neonatologist need to be aware of the potential need for respiratory support. However, the majority of these infants do well and can be delivered vaginally with no additional support required [48]. Following delivery, these infants should be assessed for respiratory stability and feeding tolerance. If stable, the infant can be discharged home. Follow-up may include radiographs

Fig. 4.6 Microcystic hybrid lung mass. (**a**) Axial US image of the fetal chest demonstrates a homogeneous echogenic mass deviating the heart to the left. Axial (**b**) and sagittal (**c**) SSFSE T2w MR confirm the presence of a high-signal right lower lobe mass. (**d**) Coronal reformatted image of a chest CT at 5 months of age demonstrates a small residual mixed cystic and solid mass in the right lower lobe. (**e**) Axial CT with intravenous contrast demonstrates the presence of a feeding systemic vessel (curved arrow) consistent with a hybrid sequestration

and CT scans, the timing of which should be dependent on whether the infant is symptomatic or not.

A recent pathologic analysis by Pogoriler et al. classified all surgically resected prenatally diagnosed lung lesions diagnosed over 2½ years [49]. In this study, lesions with large cysts (Stocker type I) were less common than those with small cysts and more likely to be symptomatic postnatally and thus need surgical management. They also found that clusters of mucinous cells are overall rare (present in 8% of congenital cystic lung lesions) but seen almost exclusively in cases with large cysts [49]. These results are useful when counseling during pregnancy.

For large masses that cause mediastinal shift and/or hydrops, delivery at a tertiary care center with an intensive care nursery capable of resuscitation of a neonate with respiratory difficulties, including capability of ECMO, should be planned [40, 46].

If the fetus is greater than 32 weeks' gestation with hydrops, delivery by EXIT should be prepared for with likely need of the mass to be resected at birth [46].

Bronchopulmonary Sequestration

Bronchopulmonary sequestration (BPS) typically has the appearance of a homogeneous triangular echogenic mass with well-defined borders by ultrasound. By definition, BPS have systemic feeding and draining vessels and consist of lung parenchyma without communication to the bronchial tree. The mass is often in the lower hemithorax adjacent to the diaphragm; most are left sided, but bilateral cases have been described [50]. Hybrid lesions can have a cystic component with feeding systemic vessels and typically have a better prognosis than patients with CPAM without systemic feeding vessels. Careful color and power Doppler assessment are critical to identify the vessel branching from the aorta below the diaphragm (Fig. 4.7). Even with careful assessment, the vascular supply may be difficult to demonstrate prenatally [32, 51].

MRI appearance is typically of a hyperintense T2w mass in the lower lobe [30, 32]. The feeding vessel may be a low-signal line coursing from the aorta into the mass. MRI does not always demonstrate the abnormal vessels but is helpful in delineating the mass, evaluating the contralateral lung, and assessing for other congenital abnormalities [32, 52]. It is particularly useful in assessing if the mass is thoracic, in the diaphragm or infradiaphragmatic. When infradiaphragmatic in location, BPS tend to be suprarenal and can mimic a neuroblastoma [32, 52].

Prognosis is favorable with only rare reports of associated hydrops. If hydrops develops after 32 weeks' gestation, early delivery is recommended. Prior to 32 weeks, in utero surgical resection or thoracentesis may be considered [53–57]. Other treatment options have been described for hydropic patients including radiofrequency ablation, laser ablation, and thrombogenic coil embolization of the feeding vessel but

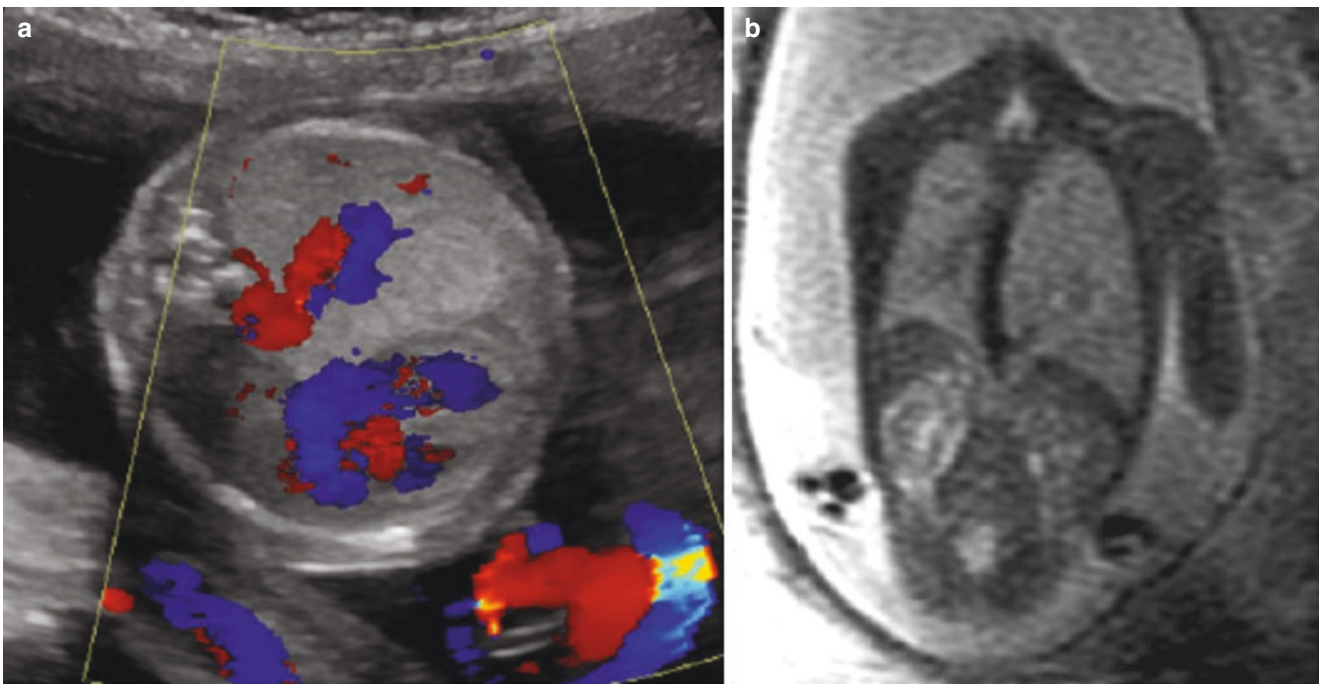

Fig. 4.7 Bronchopulmonary sequestration. (**a**) Axial US image of the fetal chest with power Doppler documents an echogenic mass in the left lung with systemic vessels coursing into the mass. (**b**) Coronal SSFSE T2w image confirms the presence of a low-signal line coursing to the high-signal mass consistent with a sequestration

thus far with increased morbidity and mortality [58, 59]. Lesions may appear to resolve in utero but are usually present on postnatal CT with contrast or MRI.

Congenital Lobar Overinflation/Congenital Lobar Emphysema/Bronchial Atresia

Intrinsic or extrinsic obstruction of the airway may result in overinflation of one or more lobes. CLO may affect one or more lobes and can be segmental or lobar. Bilateral cases have been described [60]. Criteria for the diagnosis of congenital lobar overinflation (CLO) include echogenic lung by ultrasound or high-signal T2w parenchyma with normal lung architecture and absence of macroscopic cysts. This diagnosis may be difficult to differentiate from microcystic CPAM prenatally (Fig. 4.8). The presence of normal pulmonary vascularity and lack of macrocysts can help suggest the diagnosis; confirmation is done with postnatal CT [61, 62].

By ultrasound, CLO is characterized as a homogeneous echogenic lung mass, thought to be secondary to accumulation of the pulmonary fluids within the lung due to a ball-valve mechanism occurring at the site of obstruction [60, 62]. MRI images demonstrate a homogeneous thoracic

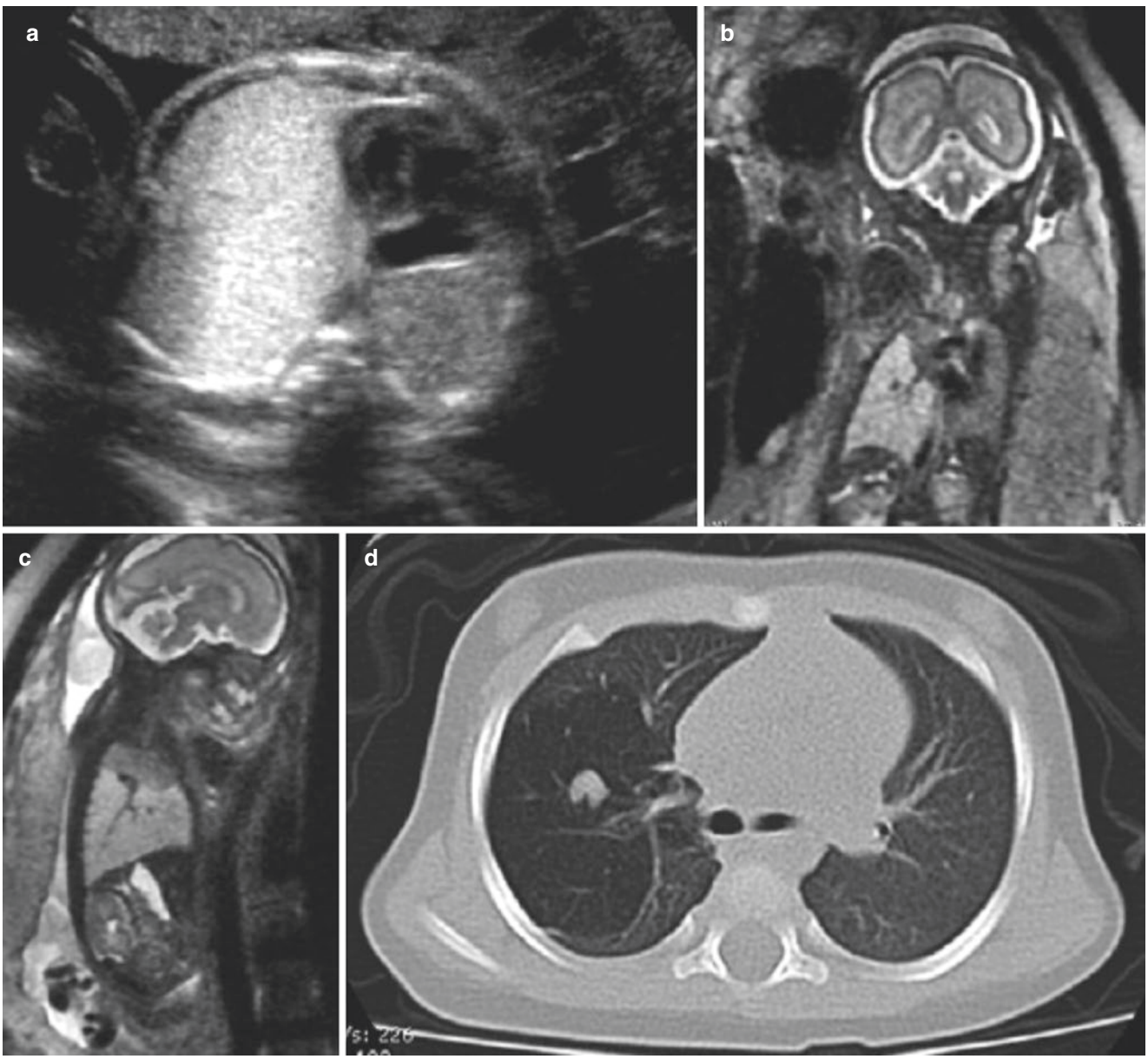

Fig. 4.8 Congenital lobar overinflation (CLO). (**a**) Axial US at 27 weeks' gestation demonstrates a large echogenic mass in the right hemithorax deviating the heart to the left. No systemic feeding vessel was identified. (**b**) Coronal and (**c**) sagittal SSFSE T2w MR image at 27 weeks gestation confirms the presence of a high-signal mass in the right lower lobe. (**d**) Axial chest CT scan at 5 months of age demonstrates an emphysematous lobe consistent with CLH

mass with increased T2 signal. Displacement of the mediastinum to the contralateral side, polyhydramnios and hydrops have been described especially secondary to bronchial atresia of lobar bronchi [61–63]. Many cases resolve in utero. When symptomatic, respiratory issues tend to occur early in life, 30% at birth, 50% in the first month, and almost all by the first 6 months of life ([60].

Diaphragmatic Hernia

Herniated bowel loops into the hemithorax can mimic a multicystic, heterogeneous lung mass by US (Fig. 4.2). Mediastinal and cardiac deviation may be the first hint that a CDH is present if the stomach remains infradiaphragmatic. When the stomach is herniated into the hemithorax, nonvisualization of stomach bubble within the abdomen is helpful for suggesting the diagnosis [32, 35]. Peristalsis of bowel loops in the thorax can sometimes be seen by ultrasound [32]. Deviation of the umbilical vein toward the side of the defect is appreciated in CDH, and an abnormal umbilical vein ratio is seen in 93% of right-sided and 98% of left-sided CDH. The umbilical vein ratio is obtained from a true axial image of the abdomen, where the umbilical vein is at its maximum lateral deviation. It is calculated by measuring the transverse diameter between the left internal rib margin and the left lateral vein edge and dividing it by the transverse diameter between the right inner rib margin and the right lateral border of the vein. This ratio is particularly useful in cases with subtle bowing, and when it is less than 0.4, it is highly predictive of liver herniation [64].

MRI helps by confirming the diagnosis, especially in right and bilateral CDH. It provides information regarding the amount of liver herniation and delineates location of small and large meconium-filled bowel in the chest. In cases with an intraabdominal stomach, it may be difficult by US to differentiate a CPAM from a CDH. MRI can easily distinguish abdominal contents within the chest from cystic lesions. MRI can provide specific information on hernia content, including the presence of the liver, size of diaphragmatic defect, and volume of ipsilateral and contralateral lung.

Congenital Hydrothorax

Pleural fluid may develop with or without an associated mass. It is considered abnormal at any gestational age and can be unilateral or bilateral.

Chylothorax is the most common cause of congenital hydrothorax and can be due to thoracic duct anomalies (Fig. 4.9). Secondary cases of hydrothorax include entities such as anemia, CPAM, BPS, lymphangiectasia, cardiac anomalies, Turner's syndrome, trisomy 21, cystic hygroma, and TORCH infection. Thus, careful assessment is required to identify associated anomalies, and karyotyping is recommended [65, 66].

Ultrasound will demonstrate anechoic fluid in the pleural space. MRI demonstrates high-signal fluid surrounding lung parenchyma and may help identify a cause for the hydrothorax such as an underlying CPAM.

Overall mortality can be as high as 50%. Natural evolution varies between spontaneous resolution and progression

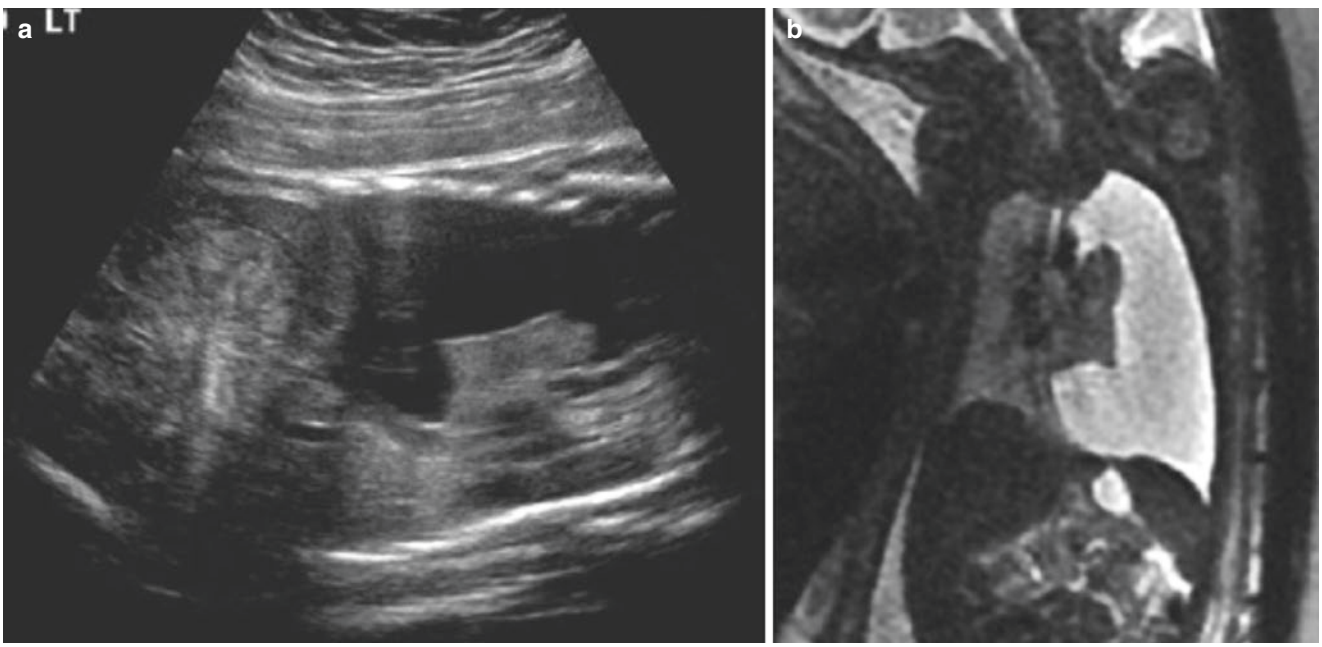

Fig. 4.9 Chylous effusion. (**a**) Coronal US of the chest demonstrates a large fluid collection in the left hemithorax compressing the left lung. (**b**) SSFSE coronal MR image confirms the presence of a large left pleural effusion with compressed lung parenchyma and no underlying lung mass

[67]. Outcome is best if the effusion is unilateral, and primary chylothorax may resolve spontaneously [65]. Prognosis is worst when hydrothorax presents before 30 weeks of gestation and is associated with hydrops [66]. If effusions progress, lung hypoplasia may occur with worsening morbidity and up to 75% mortality [67]. Patients with trisomy 21 and hydrops have a better prognosis; they can be treated later in pregnancy and require less interventions [68].

In cases with progression to hydrops, if the effusion is small, conservative observation is appropriate. If the effusion is large and the infant is less than 32 weeks' gestation, fetal thoracentesis and thoracoamniotic shunting are potential prenatal treatment options after balancing the benefits of the procedure and the possibility of prematurity and premature rupture of membranes [68]. Thoracentesis has the disadvantage of possible rapid re-accumulation after drainage but when done close to delivery may help with neonatal resuscitation [65, 68]. Complications after shunt placement also include shunt migration (20–65%), chest wall deformity secondary to altered rib growth and mechanical chest trauma during insertion (more common when shunts are placed early in gestation), and fetal demise (11% of cases) [67].

Congenital High Airway Obstruction

Congenital high airway obstruction (CHAOS) should be included in the differential when bilateral large echogenic lung masses are identified [35] (Fig. 4.10). This rare entity is usually sporadic but can be syndromic (Fraser syndrome) or as part of an association [69]. It can be secondary to laryngotracheal atresia, tracheal stenosis, or a thick web, laryngeal atresia being the most common etiology. Aberrant pulmonary budding off the foregut is present. Most cases have a connection with the esophagus. By ultrasound, both lungs are symmetrically enlarged and echogenic due to fluid trapping. The heart is compressed, usually small, and centrally located; the diaphragms flattened or inverted. Compression of the heart and great vessels may result in heart failure and hydrops. Compression of the esophagus may result in polyhydramnios [69].

MRI demonstrates abnormally large high-signal lungs on T2w that are enlarged causing eversion of the diaphragms. Identification of a dilated fluid-filled trachea and bronchi help to confirm the diagnosis and differentiate this diagnosis from bilateral CPAM. EXIT delivery with airway control is recommended but with prognosis poor [35].

Associated anomalies, such as urogenital defects, omphalocele, radial ray defects, syndactyly or polydactyly, and cryptophthalmos, should be closely looked for as this can provide useful information for future pregnancies [70]. Encephalocele and myelomeningocele have also been seen in patients with CHAOS [71]. Genetic analysis should also be performed to assess anomalies such as trisomy 9, trisomy 16, and chromosome 5p deletion [70].

Fig. 4.10 Congenital high airway obstruction. Coronal T2w MR image of the fetal chest at 27 weeks gestation demonstrates overinflated high-signal lungs with flattened diaphragms due to cervical tracheal web causing obstruction. The left bronchus is abnormally dilated with fluid. There is oligohydramnios with bilateral renal agenesis. The infant died at delivery

Pulmonary Hypoplasia

Pulmonary hypoplasia is a wide spectrum diagnosis which includes agenesis, aplasia, as well as hypoplasia. Agenesis is the actual absence of lung parenchyma and bronchi (Fig. 4.11). Aplasia is the absence of lung tissue with rudimentary bronchi. Hypoplasia is the presence of alveoli and bronchi that are underdeveloped with a decreased number of airways and alveoli resulting in a decrease in size and weight of the lungs. Alveoli and pulmonary vascularity develop concomitantly, so associated anomalies of pulmonary vessels are common.

Pulmonary hypoplasia causes severe respiratory failure at birth often resulting in rapid death. Hypoplasia can be secondary to premature rupture of membranes, renal anomalies,

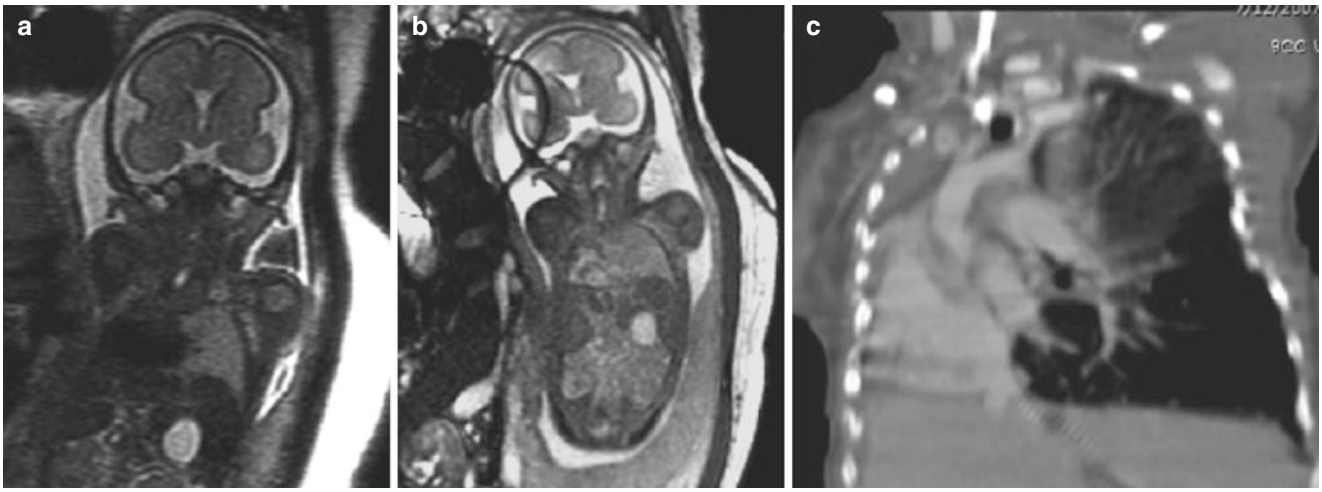

Fig. 4.11 Right lung agenesis. (**a**) Coronal SSFSE and (**b**) FIESTA T2w images at 21 weeks' gestation demonstrate shift of the heart to the right with no right lung parenchyma or right mainstem bronchus identified. (**c**) Contrast chest CT after delivery confirms the diagnosis of agenesis of the right lung

lung masses, or a severe skeletal dysplasia. Severity of the hypoplasia is dependent of gestation age at onset.

Prenatal US diagnosis of pulmonary hypoplasia is often limited. Various measurements have been proposed to predict pulmonary hypoplasia including lung area, ratio of the lung to thoracic area, thoracic to abdominal circumference, and volumetric measurements. High resistance patterns in peripheral pulmonary arteries have been reported in fetuses with pulmonary hypoplasia [72]. Both 2D diameter measurements and 3D volumetry can be performed, even before 24 weeks of gestation, for the diagnosis of hypoplasia, but follow-up assessment might be needed to assess outcome and differentiate lethal versus nonlethal forms [73]. Oligohydramnios and maternal obesity, however, limit US evaluation, so prognosis is often difficult to predict.

Fetal lung volume by MR is also being used to assess pulmonary hypoplasia [74–81] (Fig. 4.12). Relative lung volume based on gestational age and lung volume to body weight ratios have been evaluated. Normal lungs are progressively hyperintense on T2w with maturation. Decreased signal has been described in hypoplastic lungs. Relative lung signal intensity and spectroscopy are potential methods for further assessing the severity of hypoplasia [79, 80].

Several methods have been described to measure the lung volumes. One of the most common techniques is done by tracing the lung on each MRI slice, adding all the areas together, and then multiplying by the slice thickness. Using this method, normal results are highly variable. To decrease the variability, the percentage predicted lung volume (PPLV) can be used where the residual lung volume is divided by the predicted lung volume. The observed-to-expected lung volume ratio is better at predicting outcome in fetuses with CDH [82].

Fig. 4.12 Pulmonary hypoplasia. Coronal SSFSE MR image of the fetal chest demonstrates small low-signal pulmonary parenchyma in this fetus with renal anomalies resulting in oligohydramnios

Congenital Lung Tumors

Primary lung tumors are extremely rare compared to developmental anomalies of the lung and include cystic pleuropulmonary blastoma (cystic PPB), fetal lung interstitial tumor (FLIT), congenital peribronchial myofibroblastic tumor (CPMT), and congenital fibrosarcoma [83].

Even though the biological behavior of a tumor compared to a developmental anomaly is extremely different, the ability to differentiate them by imaging has been considered very difficult to impossible (Fig. 4.13). A recent study by Waelti et al. suggests that nonvisualization of a lung lesion in the mid-second trimester ultrasound should raise the concern for a tumor. In the presence of a multicystic lesion, knowledge of a normal mid-second trimester ultrasound is highly suggestive of PPB [83]. Differentiating imaging characteristics between solid tumors have not been identified.

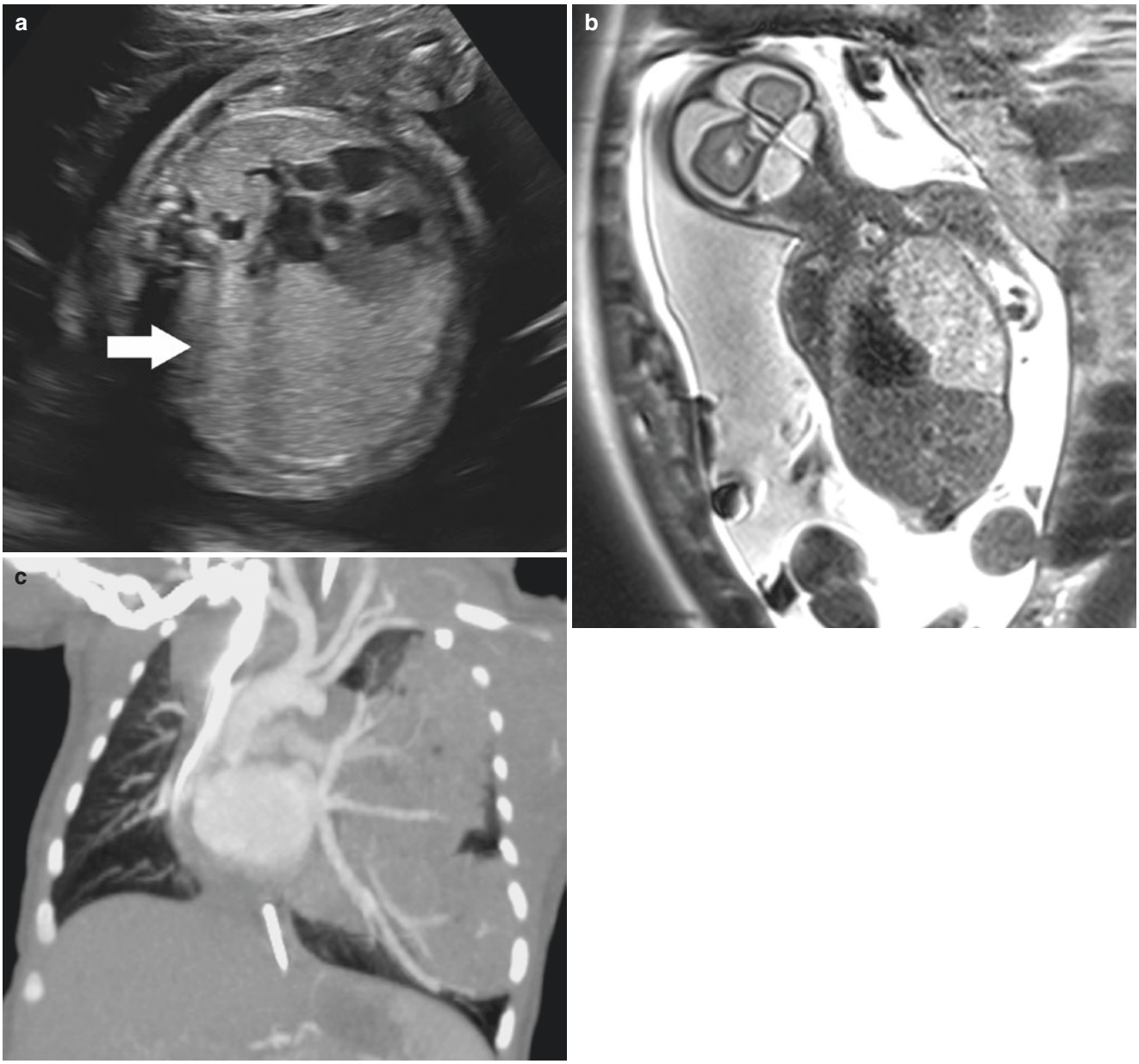

Fig. 4.13 Fetal lung interstitial tumor (FLIT). (**a**) Axial US image at 27 weeks gestation demonstrates an echogenic mass (arrow) deviated the heart to the right. (**b**) Coronal T2w MR image on the same date confirms the presence of a heterogeneous mass compressing the diaphragm inferiorly and shifting the mediastinum to the right. This was thought to be a CPAM prenatally, but the mass did not involute in the third trimester. (**c**) Following delivery, the infant was in respiratory distress. Coronal reformatted image of the chest demonstrates pulmonary vessels coursing through a solid-appearing mass. The mass was resected, and FLIT was confirmed

Pulmonary Lymphangiectasia

Pulmonary lymphangiectasia is the result of dilatation of lymphatics draining the pulmonary interstitial and subpleural spaces. This can develop prenatally resulting in enlarged, noncompliant lung parenchyma with effusions that can lead to respiratory distress at delivery [84, 85].

Lymphangiectasia can be primary or secondary. Primary pulmonary lymphangiectasia has been associated with several genetic syndromes (FOXC2) with failure of the normal regression of connective tissue elements after 16 weeks gestation. Secondary lymphangiectasia can be the result of congenital heart disease causing poor venolymphatic return. Hypoplastic left heart syndrome and total anomalous pulmonary venous return are most commonly associated with fetal lymphangiectasia [85, 86].

Prenatal ultrasound images will demonstrate small bilateral pleural effusions and heterogeneous lung parenchyma (Fig. 4.14).

Fetal MRI also can demonstrate pleural effusions and lung heterogeneity. A typical heterogeneous pattern termed the "nutmeg lung" exhibits branching tubular T2w high-signal structures radiating from the hila, providing a more specific diagnosis. MRI is also helpful in excluding other lung masses [85].

Cardiac echo is important to exclude cardiac anomalies. Not all restrictive lesions will develop the nutmeg lung pattern. In a study by Saul et al., the finding of "nutmeg lung" in fetuses with hypoplastic left heart syndrome was associated with increased mortality [87]. Fetal MRI, thus, may be a useful guide in prognosticating severity of HLHS and counseling families.

Postnatal management includes various attempts at decreasing pulmonary lymph burden such as restriction of dietary fats, pleural effusion drainage, pleurodesis, and more invasive procedures such as thoracic duct ligation. Recent experimental treatment using ethiodized oil to embolize the patulous pulmonary lymphatics has shown some success [84].

Conclusion

Congenital lung malformations are rare and often involute prenatally with a small percentage developing hydrops in utero. A majority have no respiratory symptoms at delivery. Ultrasound is the initial study to identify a congenital lung malformation which can be cystic, solid, or mixed. Fetal MRI can be a useful adjunct in the assessment of large lung masses for improved counseling and management planning. While rare, hydrops can develop with congenital pulmonary masses, is a sign of impending demise, and may be an indication for fetal intervention.

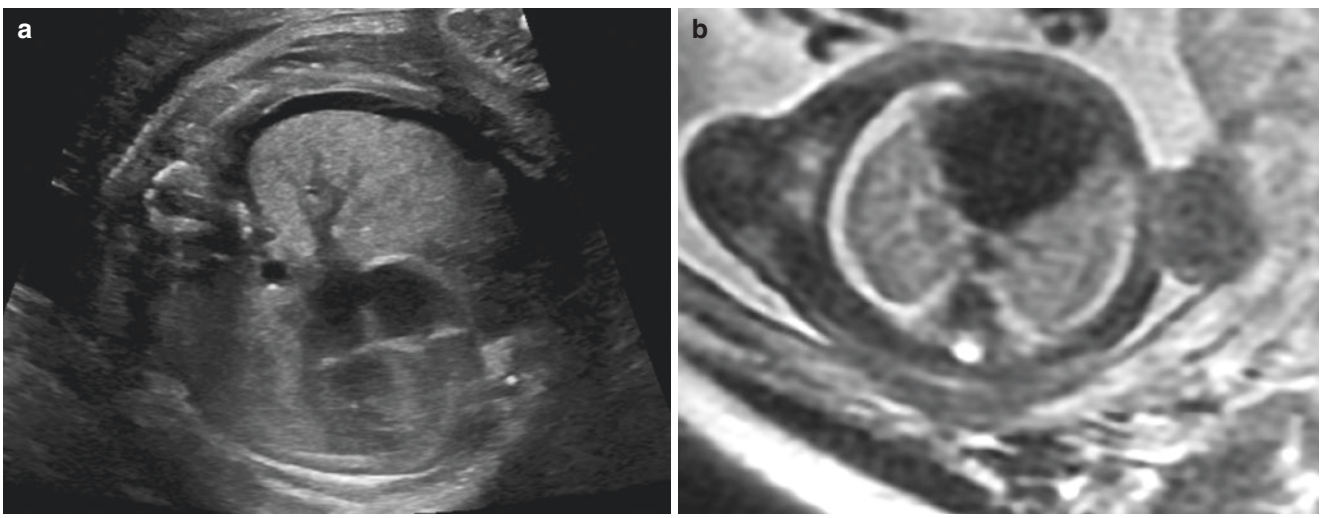

Fig. 4.14 Pulmonary lymphangiectasia. (**a**) Axial US images of the fetal chest at 28 weeks' gestation demonstrate small pleural effusions and heterogeneous parenchyma. The heart was normal. (**b**) Axial T2w MR image of the fetal chest on the same date confirms the presence of small effusions and high-signal tubular structures radiating from the hilum. At delivery primary lymphangiectasia was confirmed

References

1. Kline-Fath BM. Is prenatal sonography accurate in identification of congenital lung lesions? Scientific paper presented at SPR, Boston, MA. April 15; 2010.
2. Breysem L, Bosmans H, Dymarkowski S, et al. The value of fast MR imaging as an adjunct to ultrasound in prenatal diagnosis. Eur Radiol. 2003;13:1538–48.
3. Quinn TM, Hubbard AM, Adzick NS. Prenatal MRI enhance fetal diagnosis. J Pediatr Surg. 1998;33:553–8.
4. Bulas DI. Fetal magnetic resonance imaging as a complement to fetal ultrasonography. Ultrasound Q. 2007;23(1):3–22.
5. Aite L, Zaccara A, Trucchi A, et al. When uncertainty generates more anxiety than severity: the prenatal experience with cystic adenomatoid malformation of the lung. J Perinat Med. 2009;37:539–42.
6. Warby AC, et al. Fetal thymus and pregnant women with rheumatic disease. J Perinat Med. 2014;42(5):635–9.
7. Britto ISW, et al. New anatomical landmarks to study the relationship between fetal lung area and thoracic circumference by three-dimensional ultrasonography. J Matern Fetal Neonatal Med. 2012;25(10):1927–32.
8. Ruano R, Joubin L, Abry MC, et al. A nomogram of fetal lung volumes estimated by 3D US using the rotaional technique (virtual organ computer aided analysis). J Ultrasound Med. 2006;35:701–9.
9. Mirik Tesanic D, Merz E, Wellek S. Fetal lung volume measurements using 3D ultrasonography. Ultraschall Med. 2011;32:373–80.
10. Harmath A, Csaba A, Hauzman E, et al. Congenital lung malformations in the second trimester: prenatal ultrasound diagnosis and pathologic findings. J Clin Ultrasound. 2007;35(5):250–5.
11. Lecompte B, Hadden H, Coste K, et al. Hyperechoic congenital lung lesions in a non-selected population: from prenatal detection till perinatal management. Prenat Diagn. 2009;29:1222–30.
12. Ankerman T, Oppermann HC, Engler S, et al. Congenital masses of the lung, cystic adenomatoid malformation versus congenital lobar emphysema: prenatal diagnosis and implications for postnatal treatment. J Ultrasound Med. 2004;23:1379–84.
13. Johnson AM, Hubbard AM. Congenital anomalies of the fetal/neonatal chest. Semin Roentgenol. 2004;39:197–214.
14. Coakley FV, Glenn OA, Qayyam A, et al. Fetal MRI: a developing technique for the developing patient. AJR. 2004;182:243–52.
15. Prayer D, Brugger PC, Prayer L. Fetal MRI: techniques and protocols. Pediatr Radiol. 2004;34:685–93.
16. Baker PN, Johnson IR, Harvey PR, et al. A three year follow up children imaged in utero with echoplanar magnetic resonance. Am J Obstet Gynecol. 1994;170:32–3.
17. De Wilde JP, Rivers AW, Price DU, et al. A review of the current use of magnetic resonance imaging in pregnancy and safety implications for the fetus. Prog Biophys Mol Biol. 2005;87:335.
18. Committee of Obstetric Practice. Committee opinion no. 723: guidelines for diagnostic imaging during pregnancy and lactation. Obstet Gynecol. 2017;130(4):e210–6.
19. Yip YP, Capriotti C, Tlagala SL, et al. Effects of MR exposure at 1.5 T on early embryonic development of the chick. J Magn Reson Imaging. 1994;4:742–8.
20. Yip YP, Capriotti C, Yip JW. Effects of MR exposure on axonal outgrowth in the sympathetic nervous system of the chick. J Magn Reson Imaging. 1995;5:457–62.
21. Vadeyar SH, Moore RJ, Strachan BK, et al. Effect of fetal magnetic resonance imaging on fetal heart rate patterns. Am J Obstet Gynecol. 2000;182:666–9.
22. Mevissen M, Buntenkotter S, Loscher W. Effect of static and time varying magnetic field on reproduction and fetal development in rats. Teratology. 1994;50:229–37.
23. Ray JG, Vermeulen MJ, Bharatha A, et al. Association between MRI exposure during pregnancy and fetal and childhood outcomes. JAMA. 2016;316(9):952–61.
24. Shellock FG, Kanal E. Policies, guidelines and recommendations for MR imaging safety and patient management. JMRI. 1991;1:97–101.
25. United Nations Scientific Committee on the effects of atomic radiation. Ionizing radiation levels and effects. 1972 report to the general assembly Vol 2 effects New York; 1972.
26. Hand JW, Li Y, Thomas EL, et al. Prediction of specific absorption rate in mother and fetus associated with MRI examinations during pregnancy. Magn Reson Med. 2006;55:883–93.
27. Frates MC, Kumar AJ, Benson CB, et al. Fetal anomalies: comparison of MR imaging and US for diagnosis. Radiology. 2004;232:398–404.
28. Levine D, Barnewolt CE, Mehta TS, et al. Fetal thoracic abnormalities: MR imaging. Radiology. 2003;228:379–88.
29. Kunisaki SM, Fauza DO, Barnewolt CE, et al. Ex utero intrapartum treatment with placement of extracorporeal membrane oxygenation for fetal thoracic masses. J Pediatr Surg. 2007;42(2):420–5.
30. Daltro P, Werner H, Gasparetto TD, et al. Congenital chest malformations: a multimodality approach with emphasis on fetal MR imaging. Radiographics. 2010;30:385–95.
31. Curran PF, Jelin EB, Rand L, et al. Prenatal steroids for microcystic congenital cystic adenomatoid malformations. J Pediatr Surg. 2010;45:145–50.
32. Azizkhan RG, Crombleholme TM. Congenital cystic lung disease: contemporary antenatal and postnatal management. Pediatr Surg Int. 2008;24:643–57.
33. Adzick NS. Management of fetal lung lesions. Clin Perinatol. 2009;36:363–76.
34. Kumar AN. Perinatal management of common neonatal thoracic lesions. Indian J Pediatr. 2008;75:931–7.
35. Bush A, Hogg J, Chitty LS. Cystic lung lesions – prenatal diagnosis and management. Prenat Diagn. 2008;28:604–11.
36. Cavoretto P, Molina F, Poggi S, et al. Prenatal diagnosis and outcome of echogenic fetal lung lesions. Ultrasound Obstet Gynecol. 2008;32:769–83.
37. Stocker TJ, Manewell JE, Drake RM. Congenital cystic adenomatoid malformation of the lung: classification and morphologic spectrum. Hum Pathol. 1977;8:155–71.
38. Crombleholme TM, Coleman B, Hedrick H, et al. Cystic adenomatoid malformation volume ratio predicts outcome in prenatally diagnosed cystic adenomatoid malformation of the lung. J Pediatr Surg. 2002;37(3):331–8.
39. H Chon A, et al. A complication of percutaneous sclerotherapy for congenital pulmonary airway malformation: intravascular injection and cardiac necrosis. Fetal Pediatr Pathol. 2017;36(6):437–44.
40. Mann S, Wilson RD, Bebbington MW, et al. Antenatal diagnosis and management of congenital cystic adenomatoid malformation. Semin Fetal Neonatal Med. 2007;12:477–81.
41. Coleman BG, Adzick NS, Crombleholme TM, et al. Fetal therapy: state of the art. J Ultrasound Med. 2002;21:1257–88.
42. Morris LM, Lim FY, Livingston JC, et al. High-risk fetal congenital pulmonary airway malformations have a variable response to steroids. J Pediatr Surg. 2009;2004:60–5.
43. Kunisaki SM, Barnewolt CE, Estroff JA, et al. Large fetal congenital cystic adenomatoid malformations: growth trends and patient survival. J Pediatr Surg. 2007;42(2):404–10.
44. Knox EM, Kilby MD, Martin WL, et al. In-utero pulmonary drainage in the management of primary hydrothorax and congenital cystic lung lesion: a systematic review. Ultrasound Obstet Gynecol. 2006;28:726–34.

45. Fortunato S, Lombardo S, Dantrell J. Intrauterine laser ablation of a fetal cystic adenomatoid malformation with hydrops: the application of minimally invasive surgical techniques to fetal surgery. Am J Obstet Gynecol. 1997;177:S84.
46. Adzick NS. Open fetal surgery for life-threatening fetal anomalies. Semin Fetal Neonatal Med. 2009;15(1):1–8. (epub ahead of print).
47. Bermudez C, Perez-Wulff J, Arcadipane M, et al. Percutaneous fetal sclerotherapy for congenital cystic adenomatoid malformation of the lung. Fetal Diagn Ther. 2008;24:237–40.
48. Marshall KW, Blane CE, Teitelbaum DH, et al. Congenital cystic adenomatoid malformation: impact of prenatal diagnosis and changing strategies in the treatment of the asymptomatic patient. AJR. 2000;175:1551–4.
49. Pogoriler J, et al. Congenital Cystic Lung Lesions. Redefining the natural distribution of subtypes and assessing the risk of malignancy. Am J Surg Pathol. 2017; https://doi.org/10.1097/PAS.0000000000000992. [Epub ahead of print].
50. Hong C, Yu G, Tang J, et al. Risk analysis and outcomes of bronchopulmonary sequestrations. Padiatr Surg Int. 2017;33(9):971–5. Published online 19 June 2017.
51. Vijayaraghavan SB, Rao PS, Selvarasu CD, et al. Prenatal sonographic features of intralobar bronchopulmonary sequestration. J Ultrasound Med. 2003;22:541–4.
52. Sepulveda W. Perinatal imaging in bronchopulmonary sequestration. J Ultrasound Med. 2009;28:89–94.
53. Zeidan S, Gorincour G, Potier A, et al. Congenital lung malformation: evaluation of prenatal and postnatal radiologic findings. Respirology. 2009;14:1005–11.
54. Witlox RS, Lopriore E, Rikkers-Mutsaerts ER, et al. Single-needle laser treatment with drainage of hydrothorax in fetal bronchopulmonary sequestration with hydrops. Ultrasound Obstet Gynecol. 2009;34:355–7.
55. Oepkes D, Devlieger R, Lopriore E, et al. Successful ultrasound-guided laser treatment of fetal hydrops caused by pulmonary sequestration. Ultrasound Obstet Gynecol. 2007;29:457–9.
56. Ruano R, de A Pimenta EJ, Marques da Silva M, et al. Percutaneous intrauterine laser ablation of the abnormal vessel in pulmonary sequestration with hydrops at 29 weeks' gestation. J Ultrasound Med. 2007;26:1235–41.
57. Becmeur F, Horta-Geraud P, Donato L, et al. Pulmonary sequestrations: prenatal ultrasound diagnosis, treatment and outcome. J Pediatr Surg. 1998;33:492–6.
58. Mathis J, Raio L, Baud D. Fetal laser therapy: applications in the management of fetal pathologies. Prenat Diagn. 2015;35(7):623–36.
59. Baud D, et al. Minimally invasive fetal therapy for hydropic lung masses: three different approaches ad review of the literature. Ultrasound Obstet Gynecol. 2013;42:440–8.
60. Perea L, Blinman T, Piccione J, Laje P. Bilateral congenital lobar emphysema: staged management. J Pediatr Surg. 2017;52(9):1442–5.
61. Seo T, Ando H, Kaneko K, et al. Two cases of prenatally diagnosed congenital lobar emphysema caused by lobar bronchial atresia. J Pediatr Surg. 2006;41:E17–20.
62. Pariente G, Aviram M, Landau D, et al. Prenatal diagnosis of congenital lobar emphysema: case report and review of the literature. J Ultrasound Med. 2009;28:1081–4.
63. Peranteau WH, Merchant AM, Hedrick HL, et al. Prenatal course and postnatal management of peripheral bronchial atresia: association with congenital cystic adenomatoid malformation of the lung. Fetal Diagn Ther. 2008;24:190–6.
64. Richards DS, Kays DM. Fetal umbilical vein deviation in congenital diaphragmatic hernia. J Ultrasound Med. 2013;32:263–8.
65. Aubard Y, Derouineau I, Aubard V, et al. Primary fetal hydrothorax: a literature review and proposed antenatal clinical strategy. Fetal Diagn Ther. 1998;13:325–33.
66. Wada S, et al. The prognostic factors and outcomes of primary fetal hydrothorax with the effects of fetal intervention. Prenatal Diagn. 2017;37(2):184–92.
67. Mon RA, et al. Outcomes of foetuses with primary hydrothorax that undergo prenatal intervention (prenatal intervention for hydrothorax). J Surg Res. 2018;221:121–7.
68. Mallman MR, et al. Thoracoamniotic shunting for fetal hydrothorax: predictors of intrauterine course and postnatal outcome. Fetal Diagn Ther. 2017;41(1):58–65.
69. Gowda M, Gupta S, Ali A, Paranthaman S. Locating the level of congenital high airway obstruction: fluid in the airway tract as reference points. J Ultrasound Med. 2017;36(10):2179–85.
70. Gosavi M, Kumar L, Ratnakar A, Bannur H. Congenital High Airway Obstruction Syndrome (CHAOS): A perinatal autopsy case report. Pathol Res Pract. 2017;213(2):170–5.
71. Adin M. CHAOS associated with cervical myelomeningocele. J Clin US. 2017;45(8):507–10.
72. Chaoui R, Kalache K, Tennstedt C, et al. Pulmonary arterial Doppler velocimetry in fetuses with lung hypoplasia. Eur J Obstet Gynecol Repord Biol. 1999;84:179–85.
73. Miric TD, Merz E, Wellek S. Fetal lung volume measurements using 3DUS. Ultraschall Med. 2011;32:373–89.
74. Keller TM, Rake A, Michel SC, Seifert B, et al. MR assessment of fetal lung development using lung volumes and signal intensities. Eur Radiol. 2004;14(6):984–9.
75. Osada H, Kaku K, Masuda K, Iitsuka Y, Seki K, Sekiya S. Quantitative and qualitative evaluations of fetal lung with MR imaging. Radiology. 2004;231:887–92.
76. Tanigaki S, Miyakoshi K, Tanaka M, et al. Pulmonary hypoplasia: prediction with use of ratio of MRI measured fetal lung volume to US estimated fetal body weight. Radiology. 2004;232:767–72.
77. Ward VL, Nishino M, Hatabu H, et al. Fetal lung volume measurements: determination with MR imaging – effect of various factors. Radiology. 2006;240(1):187–93.
78. Williams G, Coakley FV, Qayyum A, et al. Fetal relative lung volume: quantification by using prenatal MR imaging lung volumetry. Radiology. 2004;233:457–62.
79. Keller TM, Rake A, Michel SC, Seifert B, Wisser J, et al. MR assessment of fetal lung development using lung volumes and signal intensities. Eur Radiol. 2004;14(6):984–9.
80. Kuwashima S, Nishimura G, Limura F, et al. Low intensity fetal lungs on MRI may suggest the diagnosis of pulmonary hypoplasia. Pediatr Radiol. 2001;31:669–72.
81. Zaretsky M, Ramus R, McIntire D, et al. MR calculation of lung volumes to predict outcome in fetuses with genitourinary abnormalities. Am J Roentgenol. 2005;185(5):1328–34.
82. Rubesova E. Why do we need more data on MR volumetric measurements of the fetal lung? Pediatr Radiol. 2016;46:167–71.
83. Waelti SL, Garel L, Soglio DD, et al. Neonatal congenital lung tumors – the importance of mid-second-trimester ultrasound as a diagnostic clue. Pediatr Radiol. 2017;47:1766.
84. Raman SP, Pipavath SN, Raghu G, et al. Imaging of thoracic lymphatic diseases. Am J Roentgen. 2009;193(6):1504–13.
85. Victoria T, Andronikou S. The fetal MR appearance of 'nutmeg lung': findings in 8 cases linked to pulmonary lymphangiectasia. Pediatr Radiol. 2014;44(10):1237–42.
86. Seed M. Antenatal MR imaging of pulmonary lymphangiectasia secondary to hypoplastic left heart syndrome. Pediatr Radiol. 2009;39:747–50.
87. Saul D, Degenhardt K, Iyoob SD, et al. Hypoplastic left heart syndrome and the nutmeg lung pattern in utero: a cause and effect relationship or prognostic indicator? Pediatr Radiol. 2016;48(4):483–9.